

Synthesis, X-Ray diffraction, Trypanocidal activity and Molecular Studies of Benzoyl Phthalimides and Isoquinolones



Paola L Ramírez-Hernandez¹, Erick Suárez-Contreras², Benjamin Noguera-Torres², Marco A. Leyva-Ramírez³, Efrén V García-Baez¹ and Marco Brito-Arias^{1*}

¹Unidad Profesional Interdisciplinaria de Biotecnología, IPN, México

²Escuela Nacional de Ciencia Biológicas, Carpío y Plan de Ayala Colonia Santo Tomás, México

³Av. Instituto Politécnico Nacional 2508, San Pedro Zacatenco, México

Submission: August 05, 2017; **Published:** August 23, 2017

***Corresponding author:** Marco Brito-Arias, Unidad Profesional Interdisciplinaria de Biotecnología, IPN, Avenida Acueducto s/n Barrio la Laguna Ticomán, 07340 México, DF, México, Email: mbrito@ipn.mx

Abstract

α -Phthalimide acetophenones **1a-b**, 3-benzoyl isoquinolones **2a-b** were synthesized by following two pathways and evaluated as trypanosol inhibitors in vitro, showing weak activity for **1a-b** and **2a**, and significant for **2b** as compared with the reference drugs benznidazol. Also docking studies were carried out to determine the binding mode, the scoring functions and the interactions with the residues at the active site of the cruzain target enzyme.

Keywords: Benzoyl isoquinolones; Trypanosoma cruzi; Molecular modeling; Phthalimide ketones; Cruzain inhibition

Abbreviations: Farnesyl Pyrophosphate Synthase (FPPS); Trans-Sialidase (TS); Trypanothione Reductase (TR); Glucose 6-Phosphate-Dehydrogenase (GPDH); Glyceraldehyde 3-Phosphate-Dehydrogenase (GAPDH); Hydroxyacid Dehydrogenase (HDH); Dimethyl Sulphoxide (DMSO)

Introduction

The development of improved drugs against parasitic diseases continues to be of high priority in some countries due their high incidence, accompanied by high toxicity treatments and therapeutic mixed results when the infection is beyond the acute and short-term phases. The protozoal infections such as Chagas disease, Leishmaniasis, and Malaria, have a significant impact in countries that are in tropical and subtropical world regions, mainly in Asia, Africa and Latin America. American trypanosomiasis or Chagas disease, caused by the hemoflagellate protozoa *Trypanosoma cruzi*, is an endemic disease in Latin America and represents a health problem estimated in 16-18 million people infected and there are 25-90 at risk of acquiring the parasite [1,2].

The current treatment against trypanosomiasis includes the nitro imidazole benznidazole, and nitrofurantoin nifurtimox which

besides the decreasing in the number of parasites, particularly benznidazole also have an effect on the motility of parasites. The therapeutic targets that have been used in the design of new drugs against Tc are: farnesyl pyrophosphate synthase (FPPS), trans-sialidase (TS), trypanothione reductase (TR), glucose 6-phosphate-dehydrogenase (GPDH), glyceraldehyde 3-phosphate-dehydrogenase (GAPDH), and α -hydroxyacid dehydrogenase (HDH) and cruzain cysteine protease [1].

The cysteine protease cruzain or cruzipain is an essential T. cruzi enzyme and one of the few validated drug targets for Chagas disease. It has a catalytic domain of 215 amino acid residues and a molecular weight of 22704 KDa. The protease is expressed in all of the stages during the life cycle of the parasite and is essential for the replication of its intracellular form [3]. Although Trypanosomiasis is considered a neglected disease,

substantial efforts have been devoted in the search of novel candidates with superior efficiency than benzimidazole and nifurtimox particularly during the chronic stage.

The use of computational database such as the online ChEMBL which perform the search based on structural and inhibition information from both functional and target assays provided valuable information for identifying compounds with known activities in *T. cruzi*. For the 2D portion of the analysis, five molecular fingerprints (Atom Pairs, Radial, MACCS keys, TGD, and piDAPH3) were generated for each structure which allowed us to rank compounds most similar to each other.

The structures with the highest scores for each fingerprint contains heterocyclic rings such as benzimidazole, benzoxazole, cumarine, phthalazine, indole, flavone, isatines, isoxazoles and quinolines [4]. Also there have been reported trypanocidal inhibitors with miscellaneous functionalities such as hydrazones [5,6] thiosemicarbazone and semicarbazone [7,8] purine carbonitriles,[9] and α -keto-based inhibitors[10] with promising results. We have previously reported the significant trypanosidal inhibition of compound **2b** and its amino derivative, and in this paper we want to make a comparative analysis of their precursors **1a-b**, **2a**.

Materials and Methods

All materials were purchased as analytical reagents, chemical solvent were distilled before use, Melting points were recorded on Fisher-Jones melting point apparatus and are uncorrected. ¹HNMR spectra were recorded at 300 MHz on a Varian spectrometer Mercury model using CDCl₃ and DMSO-d₆ as solvents. Thin layer chromatography was performed on pre-coated silica gel F254 (Merck Damstadt) with fluorescent indicator.

Chemistry

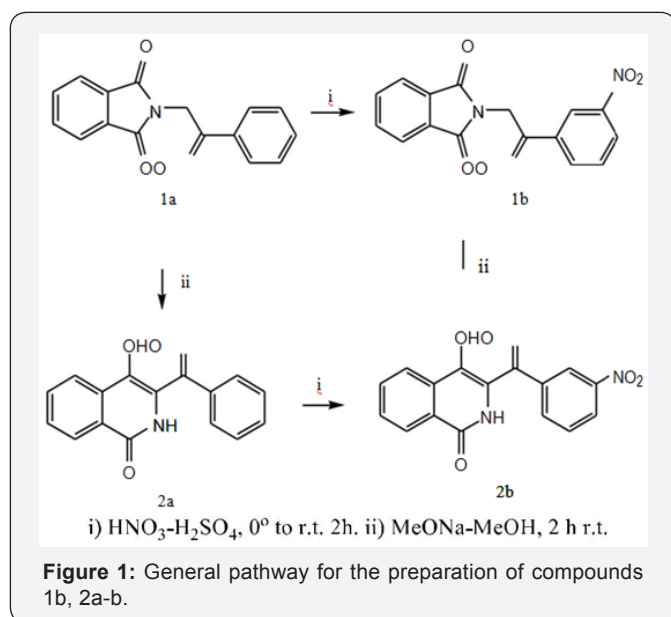


Figure 1: General pathway for the preparation of compounds **1b**, **2a-b**.

The synthesis of derivatives **1a-b**, **2a-b** was carried out according to scheme 1 starting from condensation reaction between potassium phthalimide and 2-bromacetophenone in DMF at room temperature to provide **1a** which is a common starting material for the preparation of **1b** and **2a** under nitration and basic conditions respectively. The formation of the isoquinolone nucleus proceeded via the Gabriel-Colman rearrangement [11] as it has been confirmed by x-ray diffraction [12]. Modification of the benzoyl isoquinolone **2a** at position 3 was achieved under sulfo-nitric acidic conditions affording a mixture of **2b** and **3** in 60:40 % yield (scheme 1 or Figure 1).

Experimental

2-Phthalimide-3'-nitro acetophenone (1b) In a 50 mL round bottom flask were placed compound **1a** (1.5 g, 5.65 mmol) and then cooled at 0°C. Slow addition of previously chilled solution of sulfuric acid (5 mL) was added and stirred until complete dissolution. A cold mixture of nitric-sulfuric acid (5 mL, 1:1 v/v) was added dropwise and the reaction kept at 0°C during 20 minutes allowing to reach room temperature, maintaining the stirring during further 30 minutes. The reaction mixture was poured in a beaker containing ice to induce precipitation, which was filtered, washed with distilled water (3 x 20 mL), and dried to yield 1.4 g (80 yield) of **1b** as a pale brown solid. ¹HNMR CDCl₃: δ 7.76- 7.80 (m, 3H), 7.93 (dd, 2H), 8.35 (dt, 1H), 8.52 (ddd, 1H), 8.86 (t, 1H). ¹³CNMR CDCl₃: δ 44.5, 123.3, 123.9, 128.5, 130.5, 132.2, 133.9, 134.5, 135.7, 167.9, 189.5. **3-(3-Nitrobenzoyl)-4-hydroxy-isoquinolin-1-one (2b)** In a 50 mL round flask containing compound **1b** (1g, 3.22 mmol) were cooled at 0°C and then a chilled solution of sulfuric acid (5 mL) were added and stirred until complete dissolution.

A cold mixture of nitric-sulfuric acid (5 mL, 1:1 v/v) were added slowly and the reaction kept at 0°C during 20 minutes allowing to reach room temperature, maintaining the stirring during further 30 minutes. The reaction mixture was poured in a beaker containing ice to induce precipitation, and the resulting solid filtered and washed with distilled water (3 x 20 mL) to give a mixture of **2b** which was separated by column chromatography using as elution system hexane-ethyl acetate at different concentration gradients (7:3, 5:5, 3:7) and methanol to produce 0.6 g of **2b** 60 % yield as pale yellow solid. ¹HNMR of **2b** in DMSO-d₆: δ 7.72-7.90 (m, 3H), 8.03 (d, 1H, J= 7.2 Hz), 8.11 (d, 1H, J= 6.0 Hz), 8.31 (d, 1H, J= 8.4), 8.43 (d, 1H, J= 9.6), 8.59 (s, 1H), 11.96 (s, 1H). ¹³CNMR DMSO-d₆ δ 124.2, 127.2, 127.7, 128.6, 130.9, 131.1, 133.2, 132.9, 134.8, 135.6, 135.9, 148.2, 158.0, 164.0, 166.2, 178.0.

Results and Discussion

X-Ray Diffraction of compounds **1b**

Data on compounds (**1b**) were collected on Nonius Kappa CCD diffractometer with Mo K α radiation,[13] at 298 K. The reflections were measured using combined ϕ and ω scans. The data were reduced by DENZO,[14] the structures solved using

SHELXS-97, and refined using SHELXL-97 program package [15]. ORTEP diagram was generated by ORTEP [3,16] the geometric calculations was done by PLATON[16]. All H atoms attached to C and N atoms were fixed geometrically and treated as riding with C-H=0.93Å and N-H=0.86Å with Uiso(H)=1.2Ueq(C,N). Compound (**1b**) crystallizes with two molecules in the asymmetric unit cell whose parameters are: Molecular Formula (C₁₆H₁₀N₂O₅): Mr= 310.3, triclinic, P-1, a = 7.9960(8)Å, b = 13.6480(9)Å, c = 14.92716(8)Å, α = 101.848(5)°, β = 105.577(5)°, γ = 107.115(5)°, V = 668.1(3)Å³, Z=4. ORTEP diagrams of the two independent molecules are shown in (Figure 2). As a whole the molecule is non-planar and consists of two groups, namely phthalimide and nitroacetophenone groups. The phthalimide group is planar and the bond lengths and angles are within normal ranges [17,18] The C=O bond length [C11-O11, C31-O31 = 1.220(14), 1.201 Å] is typical for arylmethylketone. The asymmetric unit consists of two crystallographically independent molecules. The dihedral angle between phthalimide and the nitroacetophenone group is 73.84(8)°. The latter is not planar with a maximum deviation of 10.03(3)° in both molecules. Bond lengths and angles are in normal ranges [19]. All hydrogen atoms were positioned geometrically and allowed to ride on their parent atoms with d(Csp²-H) = 0.93 Å or d(Csp³-H)=0.97Å and Uiso(H)=1.2Ueq(C).

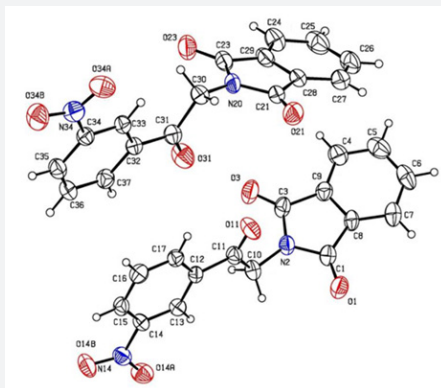


Figure 2: ORTEP representation of compound **1b** crystallizing in 2 isoforms.

Biological assays

Trypanosoma cruzi: The *T. cruzi* NINOA strain was employed in this study. This strain was isolated from an acute case of Chagas disease in the city of Oaxaca, Mexico. The parasite was maintained in the laboratory in the vector *Meccus pallidipennis* (Insecta:Hemiptera) and in female white mice.

In vitro trypanocidal assay: Compounds under study were dissolved in dimethyl sulphoxide (DMSO) at a concentration of 10 mg/mL and serial dilutions with distilled water were done to obtain the desired concentrations. All drugs and benznidazole (**Bnz**) as reference drug were evaluated against bloodstream trypomastigotes obtained by cardiac puncture of infected mice at the peak of parasitemia. Heparin was used as anticoagulant. The infected blood was diluted with sterile 0.85% saline

solution and the parasites were adjusted at 1×10^6 bloodstream trypomastigotes/mL. Bioassays were done in 96-well plates. At each well contained was added 195 μ L of the trypomastigote suspension and 5 μ L of each drug at a final concentration of 5, 10, 50, 100 μ g/mL. Control of DMSO was assayed in parallel and the concentration of DMSO never exceed 1%. The plates were incubated at 4°C for 24 h. The trypomastigotes were counted by the method described by Brener [20]. The anti-trypanosome activity was expressed as the percentage of reduction in the number of the treated parasites compared with the control (non-treated parasites). All assays were run in triplicate.

Trypanocidal activity: The compounds considered under this study (**1a-b**, **2a**) where compared with the chemotherapeutic agent of choice in the treatment of chagasic patients benznidazole (**Bnz**) which showed a lytic activity of 31% on bloodstream trypomastigotes at a concentration of 50 μ g/mL and a maximum of 46 % at 100 μ g/mL. Thus, the compounds **1a**, **1b** and **2** showed almost non observable lytic activity (Table 1).

Table 1: Anti-trypanosome activity of compounds **1a-b** and **2** in *Trypanosoma cruzi*

Concentration (μ g/mL)	Lysis of bloodstream trypomastigotes (%) of each compound			
	Bnz	1a	1b	2a
5	14	0	0	0
10	29	8	0	0
50	31	14	7	5
100	46	14	9	7

Lectures at 24 h of incubation at 4°C, Inhibition of 2b ref 4.

Docking analysis: The conformational analysis of the synthesized ligands **1a-b**, **2a-b** were carried out in order to find the best binding mode, pose and the interactions between the ligands and the residues. The program used for this study was Autodock program [21] which employs the Lamarckian algorithm and the Chimera program as visualizer system [22]. The enzyme used for the simulation was cruzain (PDB code: 1ME3) and the selected ligands were Gln19, Cys22, Ser24, Cys25, Trp26, Gly66, Asp158, His159 which are key residues present at the active site. The grid boxes have dimensions of 20 x 20 x 20, with spacing of 1.000 and x, y and z value centers of 5.417, 6.89, and 9.036. The first compound analyzed **1a** presents three rotatable with binding energy of -4.78 kcal/mol, displaying a conformation with the phthalimide moiety oriented toward the active site as shown in the ribbon and surface representations (Figure 2).

The lowest energy conformer **1a** did not show hydrogen bond interactions, however the conformation with binding energy of -2.19 showed an interaction with Cys25 (Figure 3). Ribbon and surface representation of the best pose for **1a** showing the conformation and the residues around the ligands. The docking

analysis of α -phthalimide-3-nitro-acetophenone **1b** presents four rotatable bonds with binding energy -4.29 kcal/mol for the most favored conformation having none hydrogen bond interaction with the selected residues. The ribbon and surface representation shows the ligand **1b** assuming a conformation with the phthalimide and benzoyl groups positioned in partial coplanarity without moieties embedded into the active site (Figure 4). Also it was observed a less favored conformation with binding energy of -2.2 showed hydrogen bond interaction with Gly66 (Figure 5).

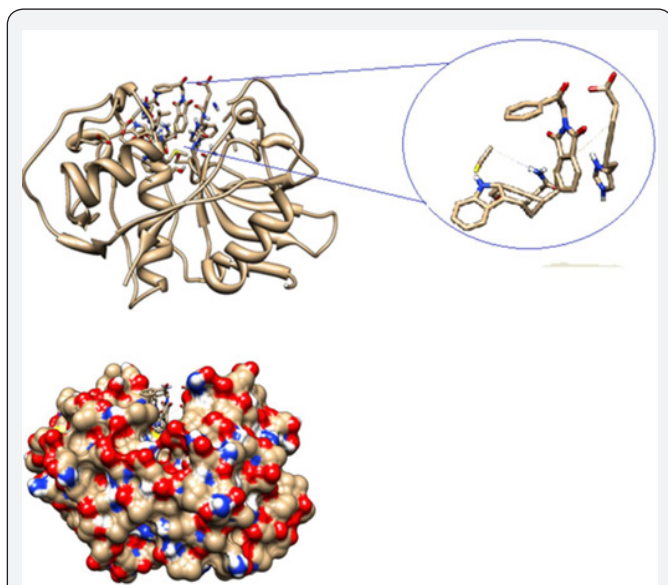


Figure 3: Ribbon and surface representation of the best pose for **1a** showing the conformation.

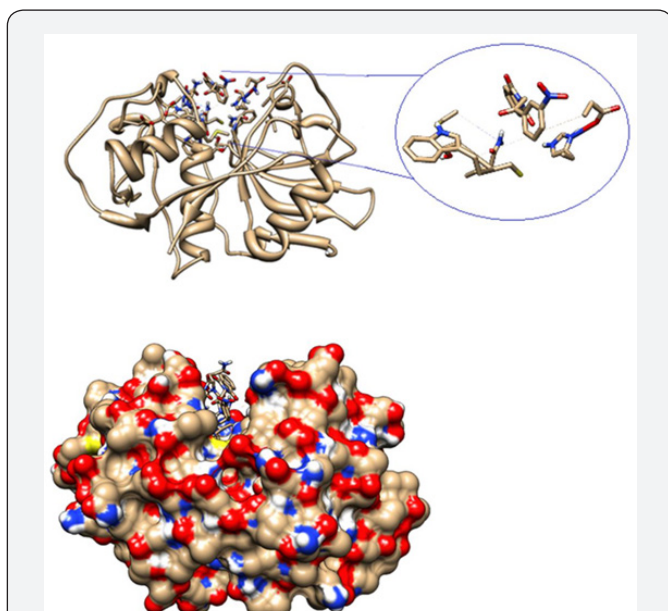


Figure 4: Ribbon and surface representation of the best pose for **1b** showing the conformation and the residues surrounding the ligands.

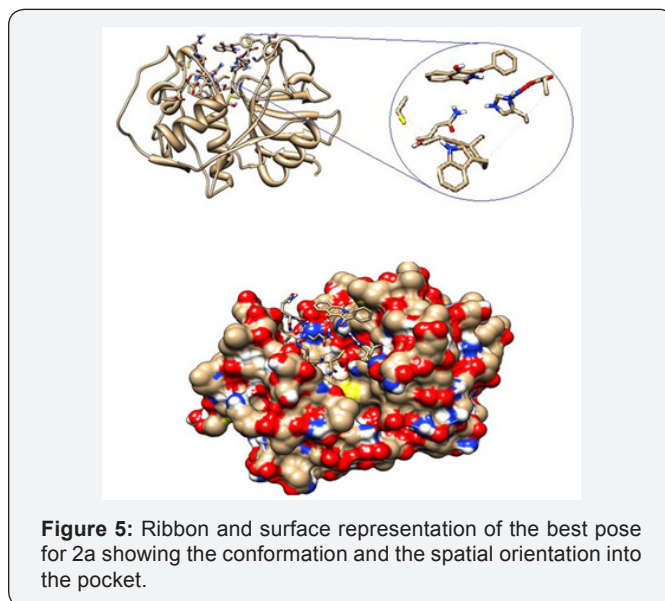


Figure 5: Ribbon and surface representation of the best pose for **2a** showing the conformation and the spatial orientation into the pocket.

Ribbon and surface representation of the best pose for **1b** showing the conformation and the residues surrounding the ligands. The docking analysis of benzoyl isoquinolone **2a** presents three rotatable bonds having a binding energy -3.99 kcal/mol, for the most favored conformation. The minimum energy orientation assumed for **2a** shows the isoquinolone moiety positioned almost orthogonal to the benzoyl fragment with none of the fragments embedded into the pocket (Figure 5). Ribbon and surface representation of the best pose for **2a** showing the conformation and the spatial orientation into the pocket. The ligand **2b** presents four rotatable bonds with binding energy of -3.04 kcal/mol, assuming a none orthogonal conformation with a binding mode opposite with **2a**, establishing a hydrogen bridge interaction between the enol group from the ligand and the carbonyl group of the residue Gly66 (Figure 6).

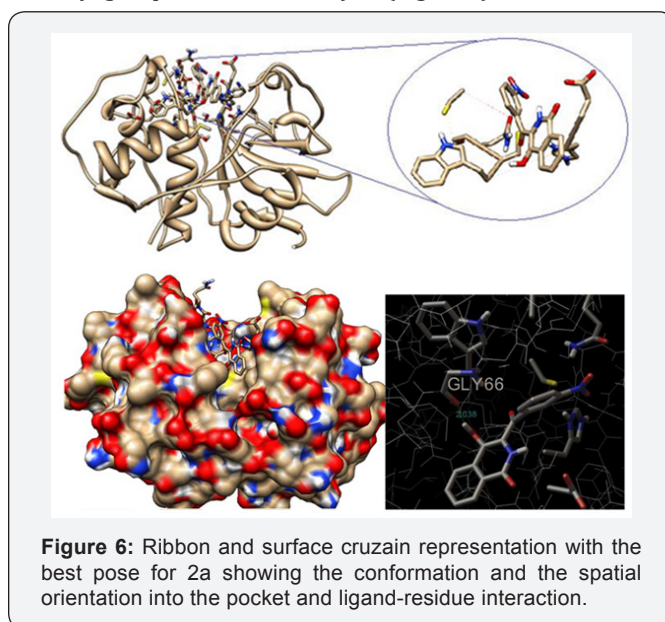


Figure 6: Ribbon and surface representation of the best pose for **2a** showing the conformation and the spatial orientation into the pocket and ligand-residue interaction.

From the docking analysis the scoring functions were determined providing low energy values indicating a likely binding interaction with the residues. However, although the binding energy and ligand efficiency for the phthalimide derivatives **1a-b** are from the same order as for the isoquinolone ligands **2a-b** and **3** the lysis was not observed. This finding can lead us to the conclusion that the phthalimide moiety is not a suitable pharmacophore for cruzain, although this statement is not conclusive considering the number of intermediates evaluated. In the case of isoquinolones derivatives **2a-b** the ligand **2b** probed to be substantially more active than the unsubstituted **2a** assuming consequently that the presence of the nitro group is critical for activity (Table 2).

Table 2: Scoring functions of compounds 1a-b, 2a-b

Entry	Binding energy kcal/mol	Ligand efficiency kcal/mol	Inhibition constant mM	Lysis % 50 µg/mL
1a	-4.78	-0.24	0.31	14
1b	-4.29	-0.19	0.71	7
2a	-3.99	-0.20	1.19	0
2b	-3.04	-0.13	5.90	47

Conclusion

We have described the synthesis, trypanocidal inhibition and comparative analysis of phthalimide acetophenones and isoquinolones, observing no trypanocidal inhibition for the phthalimide derivatives (**1a-b**) and isoquinolone **2a**, but a strong inhibition as reported previously for the nitro derivative **2b**[4]. We also described the X-ray diffraction of compounds **1b** which allowed us to analyze the conformation and hydrogen bonding interaction on the solid state and the docking studies to determine the best pose and interaction with the active site in the target enzyme cruzain.

Conflict of Interest

The authors declare that there is no conflict of interest in the preparation of this article.

Acknowledgement

MBA would like to thank Cofaa-IPN, and SIP-IPN for financial support during the development of this project.

References

- Rivera G, Bocanegra-García V, Ordaz-Pichardo C, Noguera-Torres B, Monge A (2009) New therapeutic targets for drug design against *Trypanosoma cruzi*, advances and perspectives Current Medicinal Chemistry 16(25): 3286-3293.
- Reithinger R, Tarleton RL, Urbina JA, Kitron U, Gurtler RE (2009) Eliminating Chagas disease: challenges and a roadmap. British Medical Journal pp. 338: b1283.
- McGrath ME, Eakin AE, Engel JC, McKerrow JH, Craik CS, et al. (1995) The Crystal Structure of Cruzain: A Therapeutic Target of Chagas' Disease. J Mol Biol 247(2): 251-259.
- Byler KG, Brito-Arias M, Marquez-Navarro A, Noguera-Torres B, Torres-Bustillos LG, et al. (2012) Identification of benzoylisoquinolines as potential anti-Chagas agents Bioorganic & Medicinal Chemistry 20(8): 2587-2594.
- Romeiro NC, Aguirre G, Hernández P, González M, Cerecetto H, et al. (2009) Synthesis, trypanocidal activity and docking studies of novel quinoxaline-N-acylhydrazones, designed as cruzain inhibitors candidates Bioorganic & Medicinal Chemistry 17: 641-652.
- Zanatta N, Amaral SS, dos Santos JM, de Mello DL, Fernandes LS, et al. (2008) Convergent synthesis and cruzain inhibitory activity of novel 2-(N'-benzylidenehydrazino)-4-trifluoromethyl-pyrimidines. Bioorganic & Medicinal Chemistry 16(24): 10236-10243.
- Trossini GHG, Guido RVC, Oliva G, Ferreira EI, Andricopulo AD (2009) Quantitative structure- activity relationships for a series of inhibitors of cruzain from *Trypanosoma cruzi*: Molecular modeling, CoMFA and CoMSIA studies. Journal of Molecular Graphics and Modelling 28(1): 3-11.
- Pizzo C, Faral-Tello P, Salinas G, Flo M, Robello C, et al. (2012) Selenosemicarbazones as potent cruzipain inhibitors and their antiparasitic properties against *Trypanosoma cruzi* Med Chem Commun 3: 362.
- éndez-Lucio O, Romo-Mancillas A, Medina-Franco JL, Castillo R (2012) Computational study on the inhibition mechanism of cruzain by nitrile-containing molecules Journal of Molecular Graphics and Modelling 35: 28-35.
- Choe Y, Brinen LS, Price MS; Engel JC, Lange M, et al. (2005) Development of α -keto-based inhibitors of cruzain, a cysteine protease implicated in Chagas disease. Bioorganic & Medicinal Chemistry 15: 2141-2156.
- Hill JHM (1965) Mechanism of the Gabriel-Colman Rearrangement J Org Chem 30(2): 620-622.
- Brito-Arias M, Castillo-Juárez K, Molins E (2006) 3-benzoyl-4-hydroxyisoquinolin-1(2H)-one Acta Crystallogr, Sect E: Struct Rep Online o5261.
- (1997) Nonius Kappa-CCD Server Software Nonius BV, Delft, The Netherlands, Europe.
- Otwinowski Z, Minor W (1997) Methods in Enzymology, Vol 276, Macromolecular Crystallography, Part A, edited by CW Carter Jr & RM Sweet pp. 307-326.
- Sheldrick GM (2008) A short history of SHELX Acta Cryst 64(1): 112-122.
- Farrugia LJ (1997) ORTEP-3 for Windows-a version of ORTEP-III with a Graphical User Interface (GUI) J Appl Cryst 30: 565.
- Feeder N, Jones W (1996) Structures of Five-Phthalimidoaliphatic Carboxylic Acids Acta Cryst. C52: 913-919.
- Ng SW (1992) Structure of 1H-isoindole-1, 3 (2H)-dione (phthalimide) Acta Cryst. C48 1694-1695.
- Allen FH, Kennard O, Watson DG, Brammer L, Orpen AG et al. (1987) Tables of bond lengths determined by X-ray and neutron diffraction. Part 1. Bond lengths in organic compounds J Chem Soc Perkin Trans pp. S1-19.
- Brener Z (2010) Revista do Instituto de Medicina Tropical de São Paulo, 1962(4): 389-396.
- Sanner MF, Huey R, Dallakyan S, Karnati S, Lindstrom W, et al. (2007) AutoDockTools, version 1.4.5. The Scripps Research Institute, USA.
- Pettersen EF, Goddard TD, Huang CC, Couch GS, Greenblatt DM, et al. (2004) UCSF chimera-a visualization system for exploratory research and analysis. J Comput Chem 25(13): 1605-1612.



This work is licensed under Creative Commons Attribution 4.0 License
DOI: [10.19080/OMCIJ.2017.03.555608](https://doi.org/10.19080/OMCIJ.2017.03.555608)

Your next submission with Juniper Publishers will reach you the below assets

- Quality Editorial service
- Swift Peer Review
- Reprints availability
- E-prints Service
- Manuscript Podcast for convenient understanding
- Global attainment for your research
- Manuscript accessibility in different formats
(Pdf, E-pub, Full Text, Audio)
- Unceasing customer service

Track the below URL for one-step submission

<https://juniperpublishers.com/online-submission.php>